

## Scaling Properties of Circulation in Moderate-Reynolds-Number Turbulent Wakes

K. R. Sreenivasan, A. Juneja, and A. K. Suri

*Mason Laboratory, Yale University, New Haven, Connecticut 06520*

(Received 9 January 1995)

Circulation around closed contours (square boxes) of various sizes is computed from two-dimensional spatial velocity data, acquired by the particle image velocimetry technique in the turbulent wake behind a circular cylinder. Scaling is observed for an intermediate range of box sizes even at the low and moderate Reynolds numbers of measurement. The scaling exponents are determined at various Reynolds numbers and presented with a plausible interpretation.

PACS numbers: 47.27.Ak, 47.127.Nz, 47.27.Vf

Following Kolmogorov [1], the search for universality in turbulence has usually been made in terms of velocity increments  $\Delta u_r = u(x+r) - u(x)$ , since the differencing operation is presumed to eliminate the nonuniversal large-scale effect. However, it has long been recognized [2], and explored more fully in Refs. [3] and [4], that some effects of the large scale persist well into the inertial range. Assuming that large-scale fluctuations are principally potential in nature, one can eliminate them by considering vorticity instead of velocity increments. Vorticity involves differences of velocity gradients and so, from an experimental perspective, is not amenable to accurate determination. However, once can measure with relative ease and accuracy the circulation around a closed contour  $\mathbf{l}$ , defined by the line integral

$$\Gamma_r = \oint \mathbf{u} \cdot d\mathbf{l}, \quad (1)$$

where the subscript  $r$  stands for a characteristic linear size of the contour and  $\mathbf{u}$  is the velocity vector. By Stokes theorem, circulation equals the flux of vorticity across the surface bounded by the contour. It is therefore clear that potential fluctuations do not contribute to  $\Gamma_r$ , which allows us to examine the scaling properties of the vortical part of the velocity field without measuring vorticity directly. In this Letter, we report a few characteristics of the circulation around closed contours in the turbulent wake of a circular cylinder. To our knowledge, these are the first measurements of their kind.

Three considerations prompted us to make these measurements (aside from their novelty). First, structure functions correspond to one-dimensional cuts of three-dimensional turbulence and so cannot easily recognize the contribution of filamentlike structures, while circulation can take adequate account of them. Second, Migdal [5] has calculated the probability density of circulation by working with the Hopf functional equation for three-dimensional turbulence, and it seemed useful to have an experimental counterpart to the theory. Finally, there is the attraction of obtaining some scaling properties without invoking the ubiquitous Taylor's hypothesis.

Circulation was computed from a two-dimensional velocity field acquired in a water tunnel by Suri, Juneja, and

Sreenivasan [6]. The Reynolds number,  $Re$ , based on the cylinder diameter,  $D$ , and free stream velocity,  $U_0$ , varied from 190 (just past the three-dimensional transition in the flow) to 4540 (fully developed turbulence in some respects). Table I lists some of the principal experimental conditions [7]. The velocity data were acquired using the particle image velocimetry (PIV) method. The PIV technique involves the illumination of a plane of the seeded flow field by a pair of laser pulses separated by a small but finite time interval, and the capture of both pulses on a single frame of photographic film. Each particle pair on the frame conveys information on the local velocity field. When the developed film is interrogated with a beam of He-Ne laser, the spacing and orientation of the fringes can be converted to the particle velocity at the beam location; here, this was done by using a software from FFD Inc. The accuracy of velocity data so obtained varied between 3% and 8%, with a typical value of about 5%.

The velocity vectors were obtained on a grid of size  $44 \times 66$  pixels (a pixel was 1.36 mm in some and 1.8 mm in other experiments); the grid was centered at 50 cylinder diameters downstream [10]. The pixel resolution varied from about  $2\eta$  at the lowest Reynolds number to about  $9\eta$  at the highest Reynolds number, where  $\eta$  is the estimated Kolmogorov scale. Denote  $x$  as the flow direction upstream of the cylinder,  $y$  as the direction of maximum shear, and  $z$  along the cylinder axis. Velocity data were obtained in both the transverse ( $x$ - $y$ ) and the longitudinal ( $x$ - $z$ ) planes. The  $x$ - $z$  plane is essentially homogeneous, and so results are presented for circulation in that plane. 25 independent realizations were considered for each set of

TABLE I. Some pertinent experimental variables. The fluid is water at 24 °C, and all quantities are given in cgs units.

$Re$	$U_0$	$D$	$\langle \epsilon \rangle$	$\eta/\text{pixel ratio}$
4540	31.5	1.32	14.8	9.1
3460	24.0	1.32	8.50	7.5
780	15.0	0.476	1.40	4.9
640	12.0	0.476	0.74	4.0
480	9.1	0.476	0.40	3.5
190	3.7	0.476	0.05	2.1

data. Circulation was computed for a box of a given size at all possible locations in the  $x$ - $z$  plane, and the process was repeated for all 25 realizations at a given Reynolds number. Issues of convergence of moments up to the sixth order and potential sources of uncertainty were investigated and are reported in Ref. [12]. These will be noted briefly as appropriate.

Figure 1 shows the probability density function (PDF) for the circulation around a box of linear size  $r = 8$ . (Here and elsewhere,  $r$  is expressed in pixel units, but can be converted easily to centimeters by using the data given in Table I.) This PDF is typical for boxes of linear dimension  $5 < r < 25$ , and approximately Gaussian as predicted by Migdal [5]. To understand this near-Gaussianity, note first that the circulation around a given box is equal to the sum of circulations around subboxes which make up the box and that, if  $\xi$  is the smallest box for which we can compute the circulation, one has

$$\langle \Gamma_r^2 \rangle = \sum_{i=1}^{(r/\xi)^2} \sum_{j=1}^{(r/\xi)^2} (\Gamma_\xi)_i (\Gamma_\xi)_j. \quad (2)$$

The correlation length for  $\Gamma_\xi$  is empirically observed to be of the order of four pixels, which allows us to consider that the circulation around bigger boxes arises as the sum of essentially uncorrelated subcirculations.

The above argument is rough at best, and the circulation PDF is not strictly Gaussian; the departures are especially significant for  $r < 5$ , consistent with the fact that circulation correlations are nonzero for small boxes. In fact, for

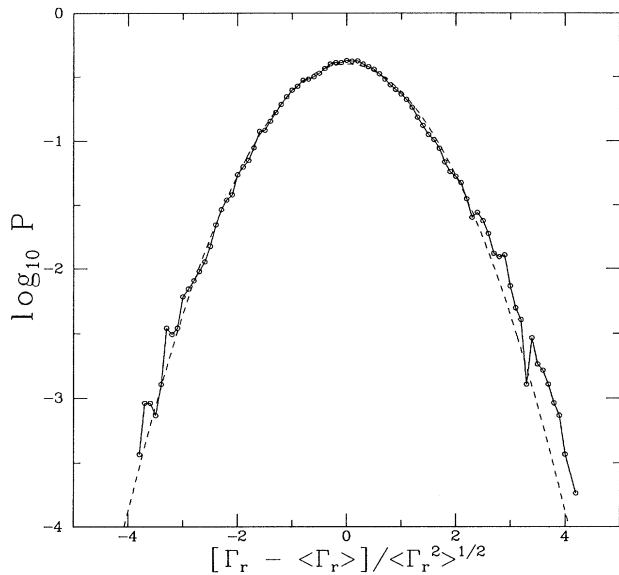


FIG. 1. The normalized PDF of circulation,  $P(\Gamma_r)$ , computed around a square box of linear dimension  $r = 8$  pixels from velocity in the  $x$ - $z$  plane of the wake obtained at  $Re = 4540$ . The mean value of circulation is very close to zero. The circulation is positive in the anticlockwise direction. The dashed line is the Gaussian distribution with the same standard deviation.

small  $r$ , the PDF approaches an exponential form. Here, we have investigated departures from Gaussianity primarily for intermediate scales, as functions of both the box size and the Reynolds number. As expected, the mean value  $\langle \Gamma_r \rangle / \langle \Gamma_r^2 \rangle^{1/2}$  was on the order of  $10^{-4}$  for all cases, and will not be discussed further. For one Reynolds number, Fig. 2 shows the moments  $\langle |\Gamma_r|^n \rangle$ , for  $n = 3, 4, 5$ , and 6, normalized suitably by the second moment, as functions of the box size; also shown for comparison are the normalized moments of the Gaussian. The circulation PDFs are modestly skewed, with a roughly constant skewness of about  $0.25 \pm 0.05$ . The fifth moment shows a greater variability with  $r$ , reaching as high a value as 2, reconfirming that the PDFs are not strictly symmetric (and hence not Gaussian either). The fourth and sixth moments also show moderate variability with  $r$ . Given the uncertainties in the moments, it is not clear if the nonmonotonic trends shown by the fifth and sixth moments can be taken seriously.

An important issue is the scaling of moments of circulation  $\langle \Gamma_r^n \rangle$  as functions of the box size  $r$ : If the PDF were strictly invariant with respect to  $r$  (e.g., exactly Gaussian), it would have been enough to consider the scaling of the variance. As seen from Fig. 2, the uncertainties are significant for the fifth- and sixth-order moments, and so the focus will be on lower moments. Since odd-order moments are small, we have considered the scaling of only the absolute value of circulation

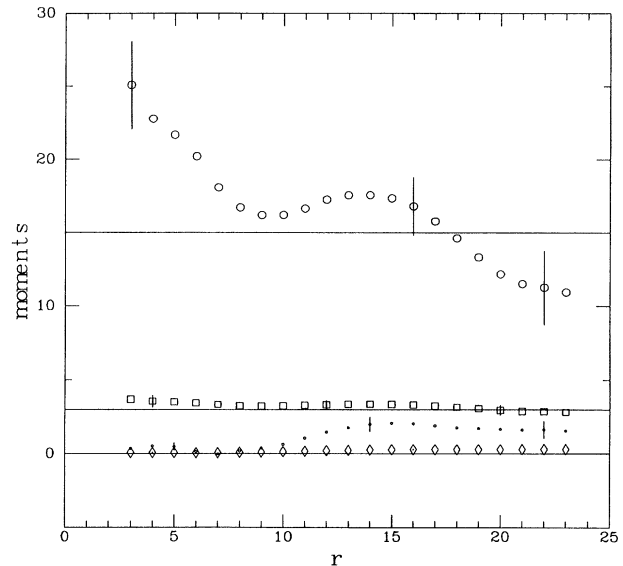


FIG. 2. Moments of circulation for  $Re = 4540$ , normalized by the second-order moment. Moments of order three (diamond), four (square), five (small circles), and six (circle) are presented. The error bars (shown here for some typical box sizes) have been determined by an assessment of the convergence of moments as a function of the sample size, as well as of how well the integrands  $\Gamma_r^n P(\Gamma_r)$  close towards the tails of  $P(\Gamma_r)$ . Details can be found in Ref. [12]. Solid lines represent Gaussian values.

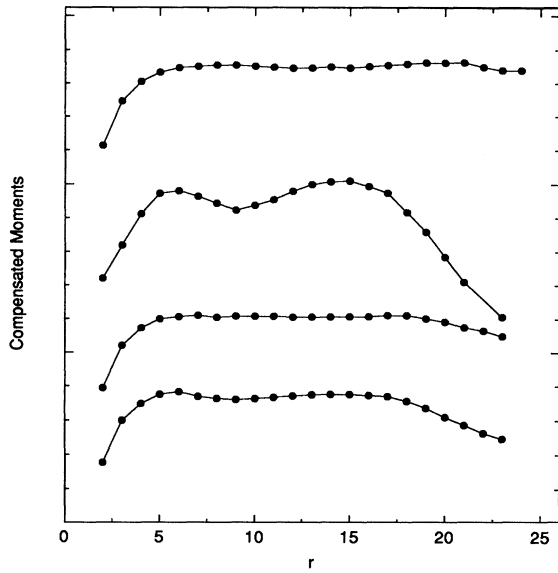


FIG. 3. Compensated moments of order 1, 2, 3, and 4 for the absolute values of circulation. The ordinates are shifted and displaced arbitrarily to avoid cluttering (from top to bottom are compensated moments of order 1, 4, 2, and 3). The scale is linear.

defined as

$$\langle |\Gamma_r|^n \rangle \sim r^{\lambda_n}. \quad (3)$$

For  $Re = 4540$ , Fig. 3 shows the compensated moments  $r^{-\lambda_n} \langle |\Gamma_r|^n \rangle$  for  $n = 1, 2, 3$ , and 4, where the  $\lambda_n$  are determined by requiring the best range of scaling for compensated moments. While a larger scaling regime would have been desirable, it is clear that the scaling is defined reasonably well. For  $Re = 4540$ , the best estimates are  $\lambda_1 = 1.13$ ,  $\lambda_2 = 2.26$ ,  $\lambda_3 = 3.38$ , and  $\lambda_4 = 4.42$ . A similar analysis of Ref. [12] suggests, although with less certainty, that  $\lambda_5 = 5.5$  and  $\lambda_6 = 6.6$ .

In general, the  $\lambda_n$  depend on the Reynolds number. We have made an extensive analysis of  $\lambda_2$  and  $\lambda_4$  at various Reynolds numbers and present the results in Table II. The best fits to data suggest that  $\lambda_6 = 3\lambda_2 - 0.5(\pm 0.1)$ , although, because of poorer scaling of the sixth moment, this statement should be treated with caution.

For the remainder, we focus on  $\lambda_2$  whose values range from about 2.04 at the lowest Reynolds number to about 2.26 at the highest Reynolds number considered here. If we note that [13]

$$\langle |\Gamma_r|^2 \rangle = r^4 \langle |\omega(r)|^2 \rangle \sim r^2 \langle (\Delta u_r)^2 \rangle \sim r^{\zeta_2 + 2}, \quad (4)$$

where the last step invokes Kolmogorov scaling for the second-order structure function [1], it follows from Eqs. (3) and (4) that

$$\lambda_2 = 2 + \zeta_2. \quad (5)$$

Data from Table I suggest that the  $\zeta_2$  would increase from about 0.04 at the lowest Reynolds number close to three-dimensional transition to about 0.26 at the Reynolds

TABLE II. Reynolds number dependence of the exponents  $\lambda_2$  and  $\lambda_4$ , inferred from the scaling of second and fourth moments of circulation. A formally meaningful error estimate is difficult to obtain but, as discussed in Ref. [12], the moments converge to within about 5%–8%.

Re	$\lambda_2$	$\lambda_4$
4540	2.26	4.42
3460	2.23	4.34
780	2.14	4.25
640	2.12	4.08
480	2.10	4.02
190	2.04	4.0

number of 4540. The Kolmogorov scaling expected to hold at high enough Reynolds number suggests the  $\zeta_2$  would approach a value of about  $\frac{2}{3}$ , implying that  $\lambda_2$  would approach a value of about  $2\frac{2}{3}$ .

Two related comments are necessary. First, when these measurements were made about four years ago, we were stymied by the fact that, even at the highest Reynolds

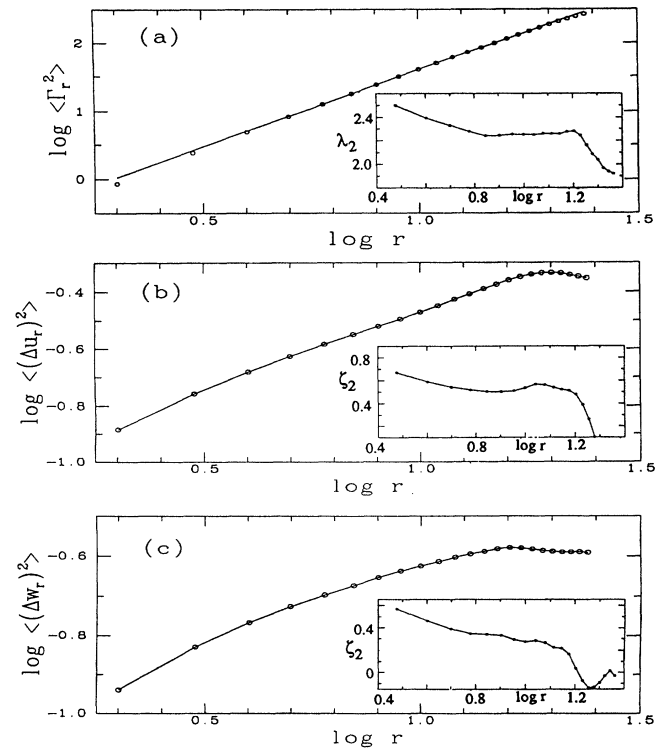


FIG. 4. Comparison of scaling of the second moment of circulation with the second-order transverse velocity structure functions from velocity data at  $Re = 4540$ . In (b) and (c),  $u$  and  $w$  are velocity components in the direction  $x$  and  $z$ , respectively, and the separation distance  $r$  is normal to the direction of the respective velocity components. Insets show local slopes. It is readily apparent that circulation has a better scaling.

number of the measurement, the exponent  $\lambda_2$  was substantially smaller than the asymptotic value of  $2\frac{2}{3}$  expected at very high Reynolds numbers. We have checked our measurements and analysis in the meantime, and confirmed the results. A possible explanation [15] for this anomaly is the anisotropy of vortex configurations caused by the large-scale shear in the flow. It has already been pointed out [16] (see caption to Fig. 6) that one effect of anisotropy in moderate-Reynolds-number shear flows is that Kolmogorov scaling applies selectively to the streamwise component of velocity, and that for it to apply to all components of velocity, much higher Reynolds numbers are needed than is usually thought.

Second, it is in principle possible to test Eq. (5) by measuring  $\zeta_2$  as well. Unfortunately, there are problems associated with such measurements at low and moderate Reynolds numbers, again a reflection of the effects of large-scale anisotropy. These are illustrated in Fig. 4. While the circulation possesses reasonably unambiguous scaling, the velocity increments at low and moderate Reynolds numbers scale less convincingly. More importantly, at these Reynolds numbers, increments of different velocity components (with separation distance normal to the direction of the velocity) scale differently. For example, we see in Fig. 4 that  $\langle(\Delta u_r)^2\rangle$  has an exponent of about 0.5 whereas  $\langle(\Delta w_r)^2\rangle$ , if there is any scaling at all, possesses a substantially smaller value.

Finally, as has been pointed out in Ref. [14], the circulation functions defined here can be thought of as generalizations of the sign-singular measure [17]. In [14], the generalized dimensions for circulation were calculated directly from the data. These numbers are in essential agreement with those inferred from the present values of  $\lambda_n$  using the formula (3.20) in [14].

These measurements were inspired by conversations with Sasha Migdal and Victor Yakhot of Princeton University in mid-1991. The manuscript has benefited significantly from useful remarks by Gustavo Stolovitzky and Samuel Vainshtein. The work was supported by a grant from the Air Force Office of Scientific Research.

[1] A.N. Kolmogorov, Dokl. Akad. Nauk SSSR **30**, 301 (1941).

[2] A.S. Monin and A.M. Yaglom, *Statistical Fluid Mechanics: Mechanics of Turbulence* (MIT Press, Cambridge,

1975), Vol. 2.

[3] P. Kailasnath, A. Migdal, K.R. Sreenivasan, V. Yakhot, and L. Zubair (to be published).

[4] L. Zubair, Ph.D. thesis, Yale University, 1993.

[5] A. Migdal (private communication).

[6] A.K. Suri, A. Juneja, and K.R. Sreenivasan, Bull. Am. Phys. Soc. **36**, 2682 (1991).

[7] Since the resolution of velocity measurements was not adequate for obtaining energy dissipation rate  $\epsilon$  accurately, it was estimated as follows. A crude estimate was first obtained from the "pseudoenergy dissipation" calculated according to the one-dimensional definition [=  $15\nu\langle(\partial u/\partial x)^2\rangle$ ], where the velocity derivative was calculated from the insufficiently resolved data. Assuming a universal form of the dissipation spectrum (see, e.g., Ref. [8]), the amount by which the dissipation was underestimated because of insufficient resolution was assessed, and a new estimate was obtained. Assuming this final value as the true energy dissipation,  $\eta$  was calculated using the definition  $\eta = (\nu^3/\epsilon)^{1/4}$ . The final dissipation estimates were comparable to those obtained using good-resolution hotwires in a similar airflow apparatus. The estimates were also comparable to those obtained from Kolmogorov's  $\frac{4}{3}$  law [9].

[8] L. Sirovich, L. Smith, and V. Yakhot, Phys. Rev. Lett. **72**, 344 (1994).

[9] A.N. Kolmogorov, Dokl. Akad. Nauk SSSR **32**, 19 (1941).

[10] It should be noted that this distance may not be far enough from the cylinder to have reached a self-preserving state [11]. However, we believe that this will not seriously affect the results and conclusions of our analysis.

[11] K.R. Sreenivasan, AIAA J. **19**, 1365 (1981).

[12] A. Juneja, Ph.D. thesis, Yale University, 1995. The thesis contains data on moments at various Reynolds numbers, figures for an Re of 190, and convergence checks and comparisons with structure functions.

[13] The subtlety involved in going from  $\omega(r)$  to  $\Delta u_r$  in Eq. (4) is discussed in Ref. [14]. Equation (3.19) of that reference is a generalization of Eq. (4) here.

[14] S.I. Vainshtein, K.R. Sreenivasan, R.T. Pierrehumbert, V. Kashyap, and A. Juneja, Phys. Rev. E **50**, 1823 (1994).

[15] A somewhat more formal but less transparent explanation, constructed in collaboration with G. Stolovitzky, can be found in Ref. [12].

[16] K.R. Sreenivasan, Proc. R. Soc. London **434A**, 165 (1991).

[17] E. Ott, Y. Du, K.R. Sreenivasan, A. Juneja, and A.K. Suri, Phys. Rev. Lett. **69**, 2654 (1992).